BJ www.biochemj.org

Biochem. J. (2012) **441**, 119–129 (Printed in Great Britain) doi:10.1042/BJ20110739

Critical roles of RNA helicase DDX3 and its interactions with eIF4E/PABP1 in stress granule assembly and stress response

Jing-Wen SHIH*, Wei-Ting WANG*, Tsung-Yuan TSAI*, Chu-Yun KUO*, Hao-Kang LI* and Yan-Hwa WU LEE*†

*Institute of Biochemistry and Molecular Biology, National Yang Ming University, Taipei 112, Taiwan, and †Department of Biological Science and Technology, National Chiao Tung University, Hsinchu 300, Taiwan

Upon environmental insults, SGs (stress granules) aid cell survival by serving as sites of translational silencing. RNA helicase DDX3 was reported to associate with SGs. However, its role in SG physiology remains undefined. We have demonstrated previously that DDX3 acts as an eIF4E (eukaryotic initiation factor 4E)-inhibitory protein to suppress translation. In the present study, we indentified the SG marker PABP1 [poly(A)-binding protein 1] as another direct interaction partner of DDX3. We established various stimuli as novel stressors that direct DDX3 with eIF4E and PABP1 into SGs, but not to processing bodies. Interestingly, down-regulation of DDX3 interfered with SG assembly, led to nuclear accumulation of PABP1 and reduced cell viability following stress. Conversely, supplementation with a shRNA (short hairpin RNA)-resistant DDX3 restored SG formation, the translocation of PABP1 into SGs and cell survival. Notably, the SG-inducing capacity of DDX3 is independent of its ATPase and helicase activities, but mapped to the eIF4E-binding region. Moreover, the eIF4E-binding-defective mutant DDX3 was impaired in its SG-inducing ability and protective effect on cell survival under adverse conditions. All together, the present study has characterized DDX3 as a pivotal SG-nucleating factor and illustrates co-ordinative roles for DDX3, eIF4E and PABP1 in integrating environmental stress with translational regulation.

Key words: DEAD box RNA helicase, DDX3, eukaryotic initiation factor 4E-inhibitory protein (eIF4E-inhibitory protein), processing body, stress granule, stress response.

INTRODUCTION

Cells have evolved multiple strategies to cope with environmental insults, such as oxidative, genotoxic, hyperosmotic and heat shock, and viral infection. The cellular response to these stresses involves a global silencing of protein translation. One hallmark of the stress response reported previously is the temporary formation of large cytoplasmic RNP (ribonucleoprotein) foci, known as SGs (stress granules) [1–3]. Although the composition may vary with stress stimuli and cell type [1,3], SGs typically harbour abortive translation initiation complexes containing polyadenylated mRNA bound to early initiation factors {such as eIF (eukaryotic initiation factor) 4E, eIF4G, eIF3 and PABP1 [poly(A)-binding protein 1]} and small ribosomal subunits. In addition to these SG core components, many other protein components, including RNA helicases, RNA-binding proteins, transcription factors, translation regulators and signalling molecules have been reported to accumulate in SGs under certain experimental conditions [1–3]. Apart from stalled translation initiation during a stress response, SG formation could be induced by pharmacological inhibition of translation initiation, knockdown of specific initiation factors, or overexpression of translational repressors [2]. However, not all initiation obstruction induces SGs, suggesting that SG assembly occurs upon certain impeded initiation processes. Most notably, SGs are highly dynamic structures and in equilibrium with translating polysomes. In addition, SGs are closely linked to another RNP granule, PB (processing body), a cytoplasmic mRNA-degradation machinery [4]. These findings therefore suggest a model in which SGs serve as triage centres that sort, remodel and export specific transcripts for re-initiation, storage or decay [1–3]. Moreover, when the cell is unable to recover from an extreme stress, SG assembly appears to provide a protective role by sequestering apoptosis-promoting factors in SGs [2]. Despite recent progress, a complete list of SG components is still lacking. Thus a deeper insight into the nature of the mRNP (messenger RNP) complex within SGs would provide a better view of their function.

Human DDX3 (also named CAP-Rf, DDX3X and DBX) is a ubiquitously expressed DEAD box RNA helicase. This family contains a highly conserved catalytic core domain that mediates the ATPase and helicase activities, as well as the less conserved N- and C-termini responsible for the specific functions of individual helicases [5,6]. DDX3 is a nucleocytoplasmic shuttling protein possessing RNA-dependent ATPase/helicase activity [7,8]. Over the last few years, DDX3 has been reported to participate various mRNA biogenesis steps, including mRNA migration [9], RNA splicing [10] and transcription [11]. Recent studies have begun to discern the involvement of DDX3 in translational control. Previously, we presented evidence that DDX3 functions as an eIF4E-inhibitory protein to specifically repress cap-dependent translation [12]. In a similar manner to other eIF4E-binding proteins, DDX3 utilizes a N-terminal eIF4E-binding consensus Y^{38}IPPHLR^{44} to interact with eIF4E. DDX3 could thereby block the formation of pre-initiation complex eIF4F and translation initiation by trapping eIF4E in a translationally inactive complex. Point mutations within this motif impair the ability of DDX3 to bind eIF4E and result in a loss of DDX3's regulatory effects on translation [12]. In addition, DDX3 may preferentially promote the translation initiation of structured 5′-untranslated regions upon its RNA helicase activity [13,14]. Interestingly, depletion

Abbreviations used: DMEM, Dulbecco's modified Eagle's medium; DTT, dithiothreitol; EGFP, enhanced green fluorescent protein; eIF, eukaryotic initiation factor; GST, glutathione transferase; mRNP, messenger ribonucleoprotein; MTT, 3-(4,5-dimethylthiazol-2-yl)-2,5-diphenyl-2*H*-tetrazolium bromide; PABP1, poly(A)-binding protein 1; PARP, poly(ADP-ribose) polymerase; PB, processing body; RNP, ribonucleoprotein; SG, stress granule; shRNA, short hairpin RNA; Sp1, specificity protein 1; TIA-1, T-cell-restricted intracellular antigen 1.

[1] To whom correspondence should be addressed (email yhwulee@nctu.edu.tw).

of DDX3 significantly reduces the protein expression of certain reporter constructs perhaps via its interaction with eIF3 [15]. These results reveal the multi-facets of mammalian DDX3 in translational control [16]. Elucidating the biological processes in which the DDX3-mediated regulation occurs may provide a detailed understanding of this DDX3-involved fine-tuning control of translation.

DDX3 has been reported to localize into cytoplasmic SGs while overexpressed or after arsenite treatment [13,17]. However, its relevance in SG physiology has not been addressed. In the present study, we initially indentified the SG marker PABP1 as another DDX3-interacting partner. As DDX3 could act as an eIF4E-inhibitory protein to repress translation [12], the interactions among DDX3 and these two SG components (eIF4E and PABP1) prompted us to investigate the functional role of DDX3 in cellular stress response. Strikingly, DDX3 is a critical factor for SG formation and cell survival following stress. Moreover, the eIF4E–DDX3 interaction is shown to be required for DDX3-mediated SG assembly and cell recovery under adverse conditions. Taken together, this study provides novel mechanistic insight into the integral roles of DDX3 and its interaction with eIF4E and PABP1 in co-ordinating translational regulation, SG dynamic and stress response.

EXPERIMENTAL

Antibodies and reagents

The following primary antibodies were used for immunoprecipitation, Western blotting or immunofluorescence: rabbit anti-DDX3 [11]; mouse anti-eIF4E (610269, BD Transduction Laboratories); mouse anti-GAPDH (glyceraldehyde-3-phosphate dehydrogenase) (G8795), mouse anti-FLAG (A8592), mouse anti-actin (A5441) (Sigma–Aldrich); rabbit anti-EGFP (enhanced green fluorescent protein) (ab6556), rabbit anti-PARP [poly(ADP-ribose) polymerase] (ab2317), goat anti-DDDDK (ab1257) (Abcam); mouse anti-PABP1 (10E10, sc-32318, Santa Cruz Biotechnology); and mouse anti-Dcp1p (H00055802-M06, Abnova) antibodies. Secondary antibodies used for immuno-fluorescence were: Alexa Fluor® 568-conjugated anti-mouse antibody (A11004), Alexa Fluor® 488-conjugated anti-mouse antibody (A11001), Alexa Fluor® 488-conjugated anti-goat antibody (A11055) and Alexa Fluor® 555-conjugated anti-rabbit antibody (A31572) (Molecular Probes). Stock solutions of sodium arsenite (Sigma–Aldrich), DTT (dithiothreitol) (Merck) and sorbitol (Sigma–Aldrich) were diluted in conditioned medium before use.

Cell culture, transfection and stress treatments

Human osteosarcoma U2OS and HeLa cervical cancer cell lines were cultured in DMEM (Dulbecco's modified Eagle's medium) supplemented with 10 % (v/v) FBS (fetal bovine serum) under 5 % CO_2 at 37 °C. Transfections were performed using the calcium phosphate method. To induce SG formation, cells were treated with various stress stimuli including sodium arsenite (0.5 mM, 30 min), sorbitol (1 M, 30 min), DTT (1 mM, 1 h), heat shock (45 °C, 45 min) and UV irradiation (10^4 μJ/cm^2) as described previously [18].

Plasmids, recombinant proteins, GST (glutathione transferase) pull-down assay and immunoprecipitation

To express GST–PABP1 and EGFP–DDX3 deletion variants, the corresponding DNA fragments of PABP1 and DDX3 were inserted between the BamHI and NotI sites of pGEX5x-1 plasmid (GE Healthcare) and the EcoRI and SalI sites of pEGFP-C2 plasmid (BD Biosciences Clontech) respectively. The integrity of each construct was verified by DNA sequencing. Plasmids pcDNA-SRα/FLAG, pcDNA-SRα/FLAG-Sp1, pcDNA-SRα/FLAG-DDX3, pcDNA-SRα/FLAG-DDX3(AAA), pcDNA-SRα/FLAG-DDX3(DQAD) and pcDNA-SRα/FLAG-DDX3(L43A), GST–DDX3 and a series of truncated DDX3 fragments have been described previously [11,12]. Knockdown of DDX3 was achieved by transfection of the pSUPER-derived plasmid expressing shRNAs (short hairpin RNAs) targeting human DDX3 (siDDX3-433/452) as described previously [19]. The pLKO.1-puro plasmid-based shRNA TRCN0000074641 (pLKO.1-shPABP1) obtained from the National RNAi Core Facility (Taiwan) was used for transient knockdown of PABP1, whereas the shRNA vector against luciferase (pLKO.1-shLuc) was used as a control for knockdown validation. The shRNA-resistant FLAG–DDX3-expressing construct was generated by using pcDNA-SRα/FLAG-DDX3 as template and introducing silent mutations (underlined) into the target sequence of siDDX3-433/452 (nucleotides 433–452, CGGCTCGAGCAGGAACTCTT) with the QuikChange® site-directed mutagenesis system (Stratagene). The purification of recombinant proteins and *in vitro* GST pull-down assay were performed in the presence of RNase A as described previously [11,12]. Immunoprecipitation was performed as described in [20] with slight modification. In brief, cell lysates (500 μg) were sonicated for 20 s in lysis buffer (0.5 % SDS, 1 % Triton X-100, 1 mM EDTA, 1 M NaCl and 20 mM Tris/HCl, pH 8.0), incubated on ice for 10 min with or without 1 mg/ml RNase A, and followed by addition of 20 μl of Protein G–Sepharose beads (GE Healthcare) conjugated with rabbit DDX3 antiserum or pre-immune rabbit serum. The beads were incubated at 4 °C for 6 h, washed three times with ice-cold PBS and subjected to Western blotting.

Immunofluorescence and laser-scanning confocal microscopy

Cells grown on coverslips were fixed in −20 °C-stored acetone/methanol (1:1) and sequentially probed with primary and secondary antibodies. After final washing, coverslips were mounted in fluorescence mounting medium (Dako), and images were captured using an Axioskop 2 fluorescent microscope (Carl Zeiss) with a CCD (charge-coupled device) camera (CoolSNAP, Photometrics). Confocal images were obtained on a Leica TCS-SP2 laser-scanning confocal microscope. Images were quantified using ImageJ software (NIH) and compiled using Adobe Photoshop software.

Cell counting and statistical analysis

For quantification, randomly selected cells were scored to determine the percentage of cells with SGs in each experiment. The number of SGs was calculated using ImageJ software. At least three experiments were conducted to obtain statistical results, presented as means ± S.D. and analysed with Student's *t* test where $P < 0.05$ was considered as significant.

Viability assay

At 48 h post-transfection, HeLa cells were stressed with either 1 M sorbitol or 1 mM arsenite for 1 h, and left to recover in normal medium for 24 h. Cell viability was then assessed by cell counting or MTT [3-(4,5-dimethylthiazol-2-yl)-2,5-diphenyl-2*H*-

tetrazolium bromide] assays, normalized to that of the control plasmid transfected cells without stress stimulation.

MTT assay and detection of apoptotic cells

The cell viability after stress treatment was evaluated using MTT. Briefly, after recovery from stress, cells were incubated with 0.5 mg/ml MTT in DMEM for 4 h at 37 °C until the formation of dark formazan crystals. After incubation with an equal volume of lysis buffer containing 20 % SDS and 50 % *N*,*N*-dimethylformamide at 37 °C for 16 h, absorbance at 570 nm was measured. Linearity of the response was examined in each experiment by measuring serial dilutions of cells. All measures were carried out in triplicate wells. Apoptotic cells were detected using the annexin V/FITC apoptosis detection kit (AVK050, Strong Biotech) according to the manufacturer's instructions.

RESULTS

DDX3 accumulated into SGs together with its interacting partners, eIF4E and PABP1, upon various environmental stresses

We have reported previously that DDX3 acts as an eIF4E-inhibitory protein to suppress translation [12]. To gain a more comprehensive understanding of this translational regulation, the immunoprecipitation was performed to identify DDX3-associated factors. The lysates prepared from HeLa cells expressing FLAG-tagged DDX3 were subjected to immunoprecipitation with anti-FLAG M2–agarose. Several proteins were identified with MS analysis, including the translation initiation factor and SG-exclusive marker PABP1. Although PABP1 was reported previously to associate with DDX3 [13], the functional role of this interaction remains uncharacterized. To verify whether DDX3 interacts directly with PABP1, a GST pull-down was conducted with bacterially expressed fusion proteins. As shown in Figure 1(A), even in the presence of RNase A, His–DDX3 was retained on the GST–PABP1-bound affinity beads, but not on the GST control resins, indicating a direct interaction between DDX3 and PABP1. Next, the interaction region of DDX3 with PABP1 was defined further by GST pull-down assay. DDX3 is characterized by a highly conserved catalytic core segment and the less conserved N- and C-termini. As shown in Figure 1(B), neither the N-terminal region ($DDX3^{1–226}$) nor the C-terminal domain ($DDX3^{535–661}$) interacted with PABP1. However, the conserved core segment ($DDX3^{227–534}$) showed a positive interaction, indicating that the central catalytic region of DDX3 is responsible for the interaction with PABP1. Notably, in our previous study, DDX3 interacts with eIF4E mainly through its N-terminal region [12]. Together, these results suggest that DDX3 could interact with eIF4E and PABP1 via different motifs.

Both PABP1 and eIF4E are known as common SG components. However, some SGs components vary with the SG-inducing stimulus [1–3]. Recently, the RNA helicases are thought to be concentrated in SGs under certain experimental conditions [2,3]. To validate further whether endogenous DDX3 is recruited to SGs together with eIF4E and PABP1 upon various stresses, we first examined the localization of DDX3 following sorbitol-induced osmotic stress. As shown in Figure 1(C), under non-stressed conditions, these three proteins were diffusely distributed throughout the cytoplasm. The sorbitol treatment induced the accumulation of DDX3 in dense cytoplasmic foci that co-localized with PABP1 or eIF4E (Figure 1C). The complex formation of endogenous DDX3 with eIF4E or PABP1 was validated further in a co-immunoprecipitation experiment shown in Figure 1(D). Sorbitol treatment has no impact on the protein levels of DDX3, PABP1 and eIF4E (Figure 1D, lower panels), and the amount of co-precipitated DDX3–eIF4E and DDX3–PABP1 complexes increased in stressed cells, but decreased in cultures during recovery (Figure 1D, upper panels), indicating that cell stress could enhance the interaction among DDX3, PABP1 and eIF4E. Treating cell extracts with RNase A before application to IgG–Sepharose had no impact on the recovery of DDX3 with PABP1 and eIF4E in sorbitol-treated cells (Figure 1D, upper panels), suggesting that these three proteins are brought together in SGs as part of a larger protein complex through the direct interactions. To address whether other cellular stresses led to the recruitment of DDX3 into SGs, HeLa cells were exposed to heat shock, endoplasmic reticulum stress induced by DTT and cytoplasmic stress induced by UV irradiation. Upon all stresses tested, endogenous DDX3 was redistributed to cytoplasmic SGs, where it co-localized with PABP1 (Supplementary Figure S1 at http://www.BiochemJ.org/bj/441/bj4410119add.htm). In addition, this relocalization of DDX3 was also observed in osteosarcoma U2OS cells under osmotic shock (Supplementary Figure S1, bottom row), revealing that DDX3 sequestration into SGs is not peculiar to HeLa cells. These results therefore indicate that DDX3 is a *bona fide* component of SGs. For simplicity, sodium arsenite and sorbitol treatments were used in subsequent experiments to induce cellular stress response.

The PBs, another kind of specific cytoplasmic foci, serve as dynamic storage compartments for mRNA decay in human cells. PBs are dynamically associated with SGs and are frequently found in close juxtaposition [4]. Moreover, SGs and PBs share certain protein components such as eIF4E, and are likely to exchange mRNPs between them [1,4]. Interestingly, the yeast homologue of human DDX3, Ded1p, localizes to PBs and affects PB formation [21]. As the PB component eIF4E interacts with DDX3, we are interested to know whether DDX3 is a constituent of the PBs and its role in PB formation. The localization of DDX3 and Dcp1a, a prominent and exclusive marker for the PBs, was compared. As shown in Figure 1(E), DDX3 is dispersed throughout the cytoplasm and no specific localization of DDX3 in PBs is detected in unstressed cells (Figure 1E, top panel). Upon induction of oxidative or osmotic stress, DDX3 is found largely excluded from Dcp1a-positive foci, indicating that DDX3 is not a component of PBs (Figure 1E, middle and bottom panels). It is worthy of note that, in these stressed cells, DDX3-containing SGs were frequently detected in close contact with PBs. A minor amount of DDX3 was particularly detectable in the interface of SG and PB (Figure 1E, middle and bottom panels, insets), suggesting a role for DDX3 in the regulated transfer of molecules occurring between SGs and PBs. Next, to study the role of DDX3 in PB formation, we conducted DDX3 overexpression or DDX3 silencing in HeLa cells, subjected these cultures to stressed or unstressed conditions, and observed the number of PBs in these cells. In each treatment, DDX3 overexpression or DDX3 silencing did not affect the formation of PBs (see Supplementary Figure S2 at http://www.BiochemJ.org/bj/441/bj4410119add.htm). Thus these results indicate that, unlike Ded1p, DDX3 does not play a significant role in PB formation.

Down-regulation of DDX3 interferes with SG assembly and induces the relocalization of PABP1 to the nucleus

To analyse the role of DDX3 in SG formation, we conducted shRNA-specific knockdown of endogenous DDX3 in HeLa cells and monitored the efficiency of SG formation under osmotic stress. Compared with the control plasmid, transient transfection of the shDDX3 construct led to a significant reduction of endogenous DDX3 expression without affecting

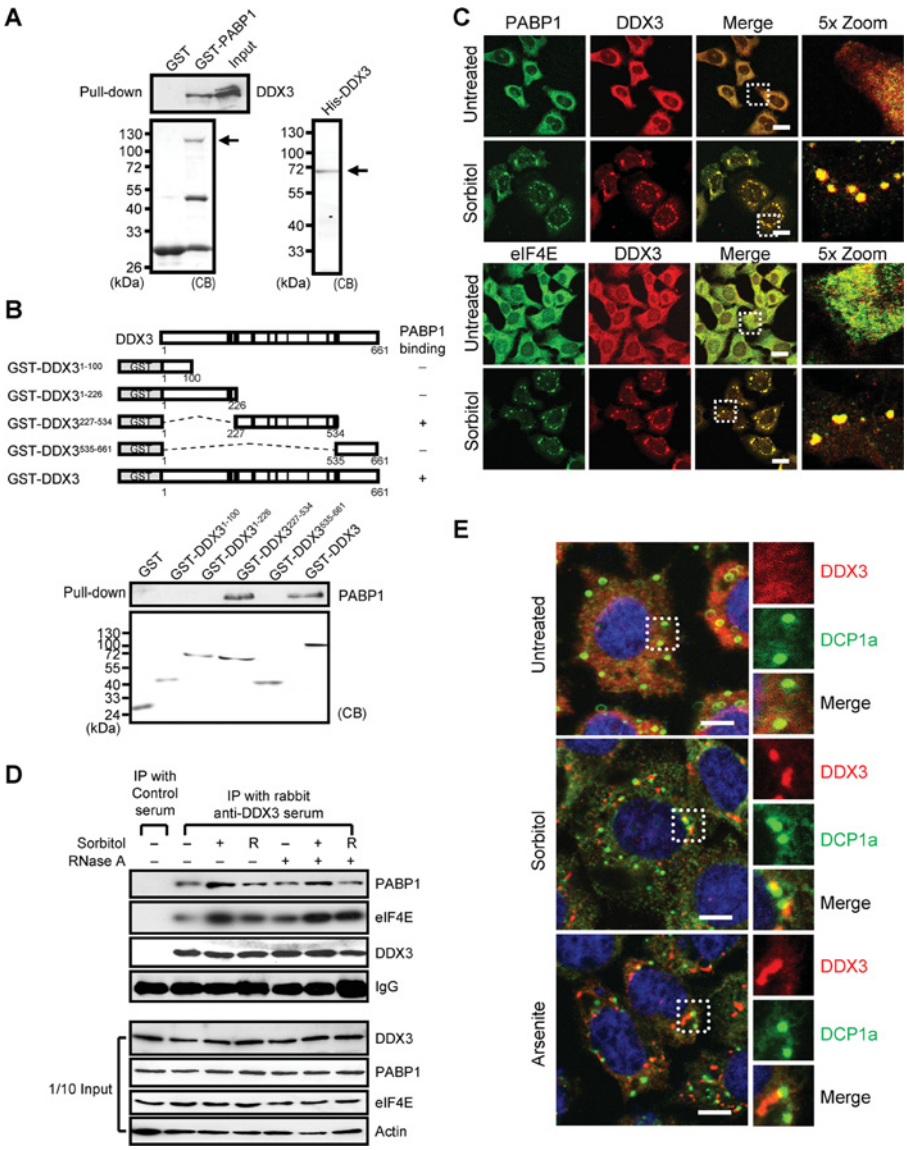

Figure 1 DDX3 and its interacting partners, eIF4E and PABP1, are co-localized to SGs upon various environmental stresses

(**A**) DDX3 interacts directly with PABP1. His–DDX3 proteins were incubated with GST or GST–PABP1 fusion proteins pre-bound on the glutathione–Sepharose beads in the presence of RNase A. After extensive washing, proteins retained on the beads were analysed by immunoblotting with DDX3 antisera. Coomassie Brilliant Blue staining (CB) of purified GST, GST–PABP1 and His–DDX3 is shown at the bottom. Molecular masses are indicated in kDa. (**B**) Mapping the interaction domain of PABP1 within DDX3. Schematic representation of GST–DDX3 variants and summary of the binding results are shown at the top. The closed black boxes indicate the position of conserved helicase functional motifs. The assays were performed by incubation of purified GST-fusion proteins with HeLa cell extracts as described above. Coomassie Brilliant Blue staining (CB) of the GST fusion proteins is shown at the bottom. Molecular masses are indicated in kDa. (**C**) The SG components PABP1 and eIF4E co-localize with endogenous DDX3 in SGs induced by osmotic stress. HeLa cells were either left untreated or treated with 1 M sorbitol for 30 min. Cells were immunostained for DDX3 together with PABP1 or eIF4E, and subsequently observed by confocal microscopy. Enlargements of boxed regions are shown in the right column. Scale bars, 20 μm. (**D**) Stress-enhanced association of DDX3 with PABP1 and eIF4E. HeLa cells were treated with or without sorbitol and followed by recovery for 6 h (R). Cell extracts collected were treated with or without RNase A before binding on to Protein G–Sepharose beads conjugated with rabbit DDX3 antiserum or pre-immune rabbit serum. The immunoprecipitates (IP) were analysed by Western blotting. A one-tenth of protein input is shown in the lower four panels. (**E**) DDX3 is not a component of PBs, but a minor amount of DDX3 is frequently detectable in the interface of SG and PB after sorbitol or arsenite treatment. HeLa cells were either left untreated or stressed with sorbitol or arsenite. After fixation, endogenous DDX3 (red) and Dcp1a (a marker of PBs, green) were detected by confocal microscopy. DAPI (4′,6-diamidino-2-phenylindole) staining of nuclei (blue) is also shown in the merged images. The indicated insets were reproduced as amplified replicate views of the same fields. Scale bars, 10 μm.

the expression of eIF4E (Figure 2A, immunoblotting). These transfected cells were then treated with sorbitol and analysed for SG formation. Using anti-eIF4E antibodies, we quantified the number of microscopically detectable SGs in these cells. As shown in Figure 2(A), DDX3-silenced cells (indicated by arrows) formed much fewer eIF4E-positive SG foci, compared with the inefficiently silenced cells (indicated by arrowheads) in the same culture or the control vector-transfected cells under the identical stress condition. To validate this result, we employed HeLa cultures co-transfected with shDDX3 construct and shRNA-resistant FLAG–DDX3-expressing plasmid to determine whether SG formation could be recovered by re-expressing DDX3. Quantification data confirmed that the significantly reduced SG-positive cell counts in DDX3-silencing cultures (from 95 to 59 %, Figure 2A) could be enhanced by the expression of shRNA-resistant FLAG–DDX3 (from 59 % to 87 %, Figure 2A).

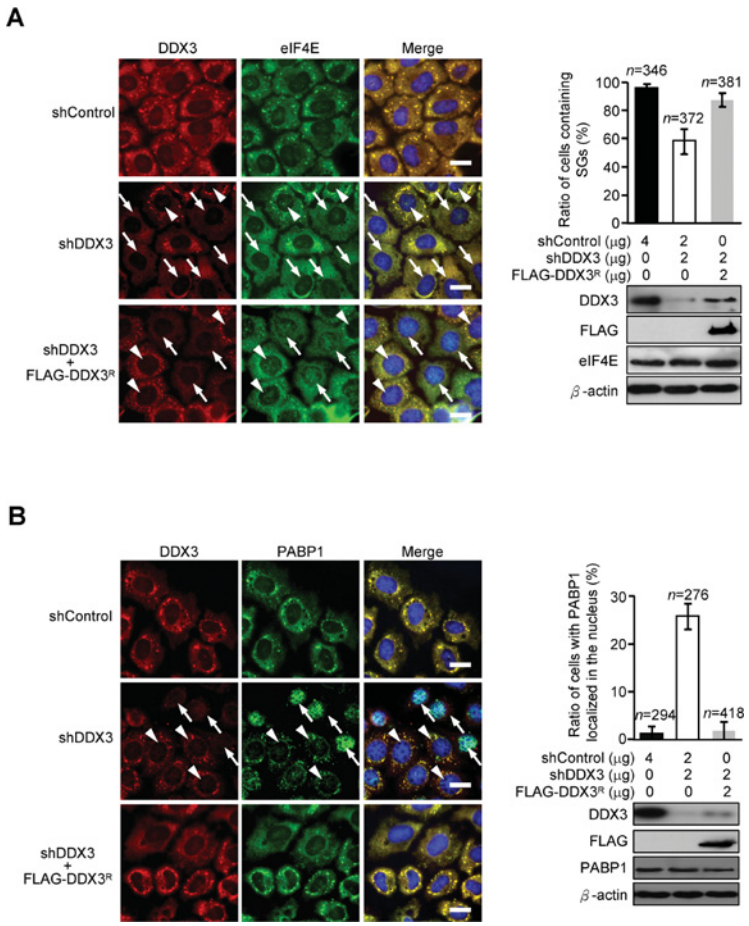

Figure 2 Silencing DDX3 impairs SG assembly and causes the relocalization of PABP1 to the nucleus

(**A**) Immunohistochemistry of eIF4E and DDX3 in HeLa cells transfected with control vector (shControl), DDX3-silencing plasmid (shDDX3) or shDDX3 with a shRNA-resistant FLAG–DDX3-expressing vector (FLAG–DDX3^R) after sorbitol treatment. Efficiently and inefficiently silenced cells are marked by arrows and arrowheads respectively. Down-regulation of DDX3 was examined by immunoblotting. DAPI (4′,6-diamidino-2-phenylindole) staining of nuclei (blue) is also shown in the merged images. Quantification of cells containing eIF4E-positive SGs under sorbitol stress is shown on the right. (**B**) Silencing DDX3 induces the relocalization of PABP1 into the nucleus. Immunohistochemistry of PABP1 and DDX3 in HeLa cells transfected with the indicated plasmids after sorbitol treatment are shown. Efficiently and inefficiently silenced cells are marked by arrows and arrowheads respectively. The nucleus is shown in blue in the merged images by DAPI staining. Down-regulation of DDX3 was examined by immunoblotting. Quantification of cells with PABP1 localized in the nucleus is shown on the right. Scale bars, 20 μm. (*n*, the number of cells used for quantification)

In addition, a similar result was also observed by using antibody against PABP1, whereas PABP1 levels remained unaffected upon DDX3 knockdown (Figure 2B, immunoblotting). Notably, the distribution of PABP1 changed more dramatically, from the cytoplasm to the nuclei of the cells (Figure 2B). Quantification data showed that DDX3 down-regulation significantly induces the translocation of PABP1 from the cytoplasm to the nuclei of the cells after sorbitol treatment (Figure 2B, from 1.2 to 25.6 %). However, neither sorbitol treatment nor DDX3 knockdown alone could induce this relocalization of PABP1 into the nuclei (see Supplementary Figure S3 at http://www.BiochemJ.org/bj/441/bj4410119add.htm). In addition, knockdown of PABP1 had no obvious effect on SG formation (see Supplementary Figure S4 at http://www.BiochemJ.org/bj/441/bj4410119add.htm), suggesting that the scarcity of cytoplasmic PABP1 is not the primary cause of this DDX3-knockdown-induced interference of SG formation. Most remarkably, this nuclear accumulation of PABP1 induced by DDX3 knockdown could be reduced upon supplementation with shRNA-insensitive FLAG–DDX3 (1.8 %, Figure 2B). Thus these results reveal a critical role of DDX3 in the function and biogenesis of SGs.

Even in the absence of stress, several SG nucleators, such as G3BP [Ras-GAP SH3 (Src homology 3) domain-binding protein], TIA-1 (T-cell-restricted intracellular antigen 1) and TIAR (TIA-1-related protein), can assemble SGs upon overexpression [1]. In agreement with the previous study conducted with GFP–DDX3 [13], overexpression of FLAG–DDX3 alone could induce the assembly of PABP1-containing SGs without stress stimuli (see Supplementary Figure S5A at http://www.BiochemJ.org/bj/441/bj4410119add.htm). Notably, the percentage of FLAG–DDX3 transfectants exhibiting spontaneous SGs increases with the expression levels of ectopic DDX3 (see Supplementary Figure S5B). This DDX3 concentration-dependent SG induction indicates that DDX3 is another SG-nucleating factors. Collectively, it is concluded that DDX3 has an active role in stimulating SG formation and maintaining SG integrity.

The ability of DDX3 to induce SG assembly is independent of its ATPase and helicase activities

DDX3 harbours ATPase and helicase activities with profound effects on its diverse biological activities [11,13]. We therefore

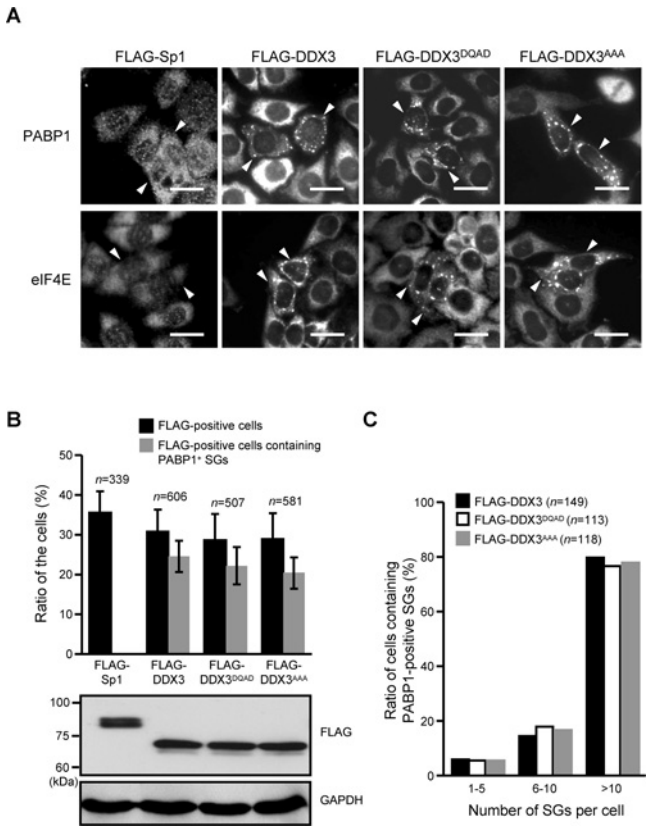

Figure 3 The ability of DDX3 to induce SG assembly is independent of its ATPase and helicase activities

(**A**) FLAG-tagged Sp1, DDX3, DDX3^{DQAD} or DDX3^{AAA} was transiently expressed in HeLa cells. Immunostaining was performed using antibodies against PABP1 or eIF4E. Counterstaining with anti-FLAG antibody is shown in Supplementary Figure S6 at http://www.BiochemJ.org/bj/441/bj4410119add.htm. The transfected cells (FLAG-positive) are marked by arrowheads. Scale bars, 20 μm. (**B**) Three independent immunofluorescence analyses showing the percentage of transfected cells (FLAG-positive) and the ratio of the transfected cells harbouring PABP1-positive SGs are quantified. Proteins in total cell lysates were subjected to immunoblotting using antibodies against the indicated proteins. (*n*, the number of cells used for quantification). Molecular masses are indicated in kDa. (**C**) The number of PABP1-positive SGs per cell was counted in the indicated plasmid-transfected cells harbouring SGs (*n*, the number of FLAG-positive cells harbouring SGs used for quantification).

examined the roles of these two enzyme activities on the SG-inducing ability of DDX3 by introducing point mutations into DDX3. A point mutation of the DEAD motif to a DQAD sequence severely impairs ATPase activity and helicase activity, whereas the conversion of the SAT motif into AAA leads to a loss of the RNA-unwinding activity, but retains the ATPase activity of the helicase [11,22]. As shown in Figure 3(A), overexpression of FLAG–DDX3^{DQAD} and FLAG–DDX3^{AAA} mutants induced PABP1- and eIF4E-containing SG assembly without stress treatment (counterstaining with anti-FLAG antibody is shown in Supplementary Figure S6 at http://www.BiochemJ.org/bj/441/bj4410119add.htm). This SG induction was not due to transfection conditions or overloading of translation machinery, as overexpression of FLAG–Sp1 (specificity protein 1) in a similar manner failed to stimulate SG formation (Figure 3A). Notably, compared with the wild-type FLAG–DDX3, overexpression of these two mutants neither affected the ratio of the cells harbouring PABP1-positive SGs (Figure 3B) nor had any significant effect on the number of PABP1-positive SGs (Figure 3C). This suggests that these two enzymatic activities have no critical role in the SG-inducing ability of DDX3.

Characterization of DDX3 domains required for SG aggregation and recruitment

We next investigated which region of the DDX3 protein is responsible for the induction of SGs. Plasmids encoding several EGFP-tagged truncation mutants of DDX3 were constructed (Figure 4A). We transfected HeLa cells with these constructs, verified their expression (see Supplementary Figure S7 at http://www.BiochemJ.org/bj/441/bj4410119add.htm), and scored the translocation of EGFP–DDX3 variants into SGs by PABP1-immunostaining. As shown in Figure 4(B), transfections of DDX3 and DDX3$^{1–534}$ induced SG formation in 58 % and 53 % of transfected cells respectively, indicating that the C-terminal region of amino acids 535–661 of DDX3 is dispensable for SG induction. Interestingly, overexpression of DDX3$^{227–534}$ showed little SG assembly (2 %), suggesting the importance of the N-terminus of DDX3 in SG induction. Consistently, the overexpression of DDX3$^{1–100}$ and DDX3$^{1–226}$ were capable of inducing SG formation. However, the SG-inducing ability of these N-terminal fragments is insufficient compared with that of the full-length proteins, suggesting that the interactions with both eIF4E and PABP1 are required for the efficient SG-inducing capability of DDX3. All together, these results indicate that, under resting conditions, the SG-induction ability of DDX3 is mapped to its N-terminal region of amino acids 1–100.

Moreover, to determine which motifs are responsible for DDX3 recruitment into SGs under stress, cells were transfected with the same constructs, treated with sorbitol and scored for the translocation of EGFP–DDX3 variants into PABP1-positive SGs (Figure 4C). After induction of stress, DDX3 and DDX3$^{1–534}$ were found in discrete PABP1-positive foci in most of transfected cells, revealing that the deletion of the C-terminal domain of DDX3 did not affect the capability of the recombinant protein to migrate into SGs (Figure 4C, 89 % compared with 76 %). In contrast, the deletion of the N-terminal region of amino acids 1–226 of DDX3 abolished the recruitment of EGFP–DDX3 into SGs (Figure 4C, 0.7 %), suggesting that this domain is necessary for recruitment of DDX3 into SGs. We tested further whether the N-terminus of DDX3 could independently promote the accumulation of EGFP in the SGs. As shown in Figure 4(C), both DDX3$^{1–100}$ and DDX3$^{1–226}$ are sufficient to bring EGFP into granules (30 % compared with 29 %), although the ability of these fragments to concentrate in the granules is insufficient compared with that of the full-length proteins. These data demonstrate that the stress-induced accumulation of DDX3 in SGs is mainly linked to its N-terminal region of amino acids 1–100. Remarkably, DDX3 interacts with eIF4E and PABP1 through its N-terminus [12] and central core region (Figure 1B) respectively. Thus these results may suggest that the DDX3–eIF4E interaction is critical for DDX3-mediated SG formation, whereas the association between DDX3 and PABP1 may have little effect during these processes.

The eIF4E–DDX3 interaction is critical for the ability of DDX3 to induce SG assembly

As the N-terminus of DDX3 harbouring the conserved eIF4E-binding motif is sufficient and essential for its SG-induction ability (Figure 4), these findings prompted us to investigate the relevance of this eIF4E–DDX3 interaction to the SG-inducing ability of DDX3. Previously, we have reported that a DDX3 mutant with a L43A point mutation is impaired in its ability to

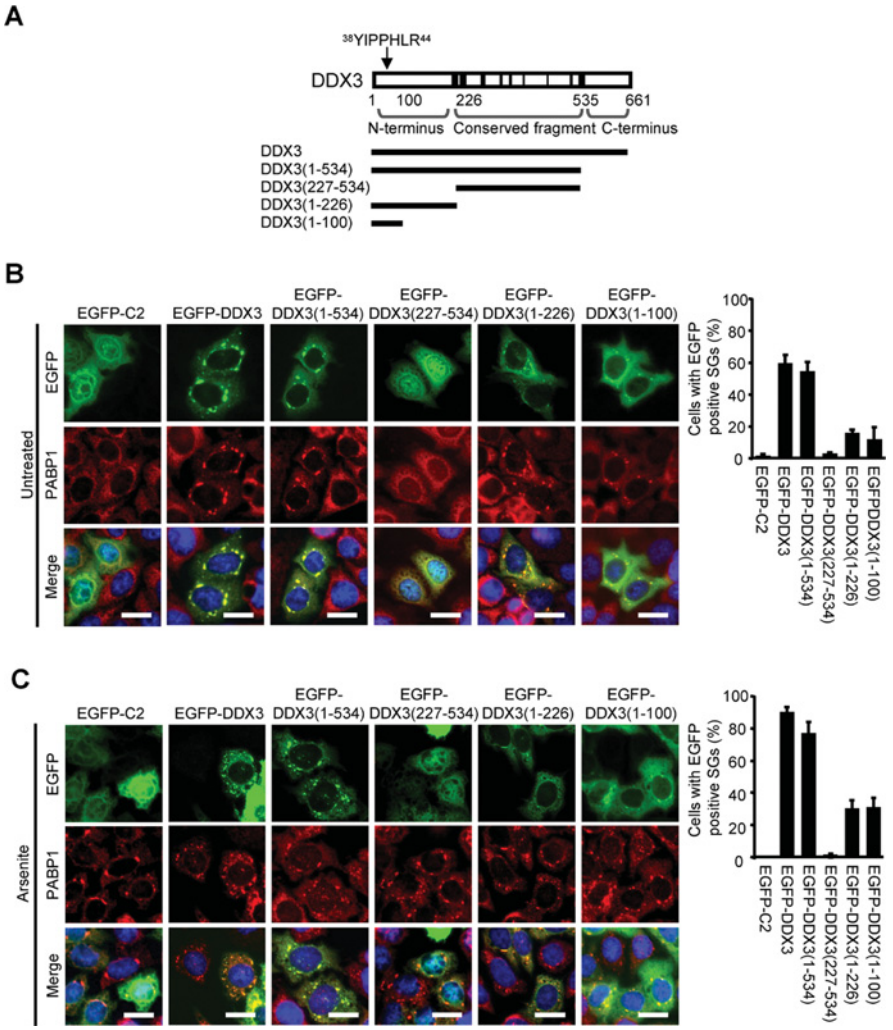

Figure 4 The N-terminal domain of DDX3 is essential and sufficient for its localization in SGs

(**A**) Schematic representation of EGFP–DDX3 variants. The relative positions of the eIF4E-binding consensus and the spaced helicase functional motifs (indicated by the closed black box) in DDX3 are also shown. (**B**) Mapping of DDX3 domains required for induction of SG assembly. HeLa cells were transfected with the indicated plasmids. After 48 h, cells were fixed and immunostained for PABP1. DAPI (4′,6-diamidino-2-phenylindole) staining of nuclei (blue) is also shown in the merged images. Three independent immunofluorescence analyses showing the percentage of transfected cells with EGFP signals detected in SGs are quantified. (**C**) Mapping of DDX3 domains required for migration to SGs. HeLa cells were transfected with the indicated plasmids. After sorbitol treatment, cells were fixed, immunostained and analysed as described above. Scale bars, 20 μm.

bind eIF4E [12]. Thus HeLa cells expressing wild-type FLAG–DDX3 or eIF4E-binding-defective mutant FLAG–DDX3^{L43A} were analysed for SG assembly by immunostaining for FLAG with PABP1 or eIF4E. As shown in Figure 5(A), overexpression of FLAG–DDX3 and FLAG–DDX3^{L43A} mutant induced PABP1- and eIF4E-positive SG assembly (counterstaining with anti-FLAG antibody is shown in Supplementary Figure S8 at http://www.BiochemJ.org/bj/441/bj4410119add.htm). Overexpression of FLAG–Sp1 in a similar manner serves as a control to exclude the possible SG induction caused by transfection conditions or overloading of translation machinery (Figure 5A). Notably, quantification of the transfected cells harbouring PABP1-positive SGs showed that DDX3^{L43A} mutant significantly reduced the number of cells forming SGs from 26.7 % to 9.9 % (Figure 5B). Furthermore, in these transfected cells harbouring SGs, the number of cells with fewer than five SGs rose from 9 % (wild-type) to 70 % (DDX3^{L43A}), whereas the number of cells with more than ten SGs decreased from 78 % (wild-type) to 11 % (DDX3^{L43A}) (Figure 5C). In addition, as the interaction between eIF4E and DDX3^{L43A} is not fully disrupted [12], this weak association may account for the residual SG formation induced by DDX3^{L43A} overexpression. Collectively, these findings revealed that the DDX3^{L43A} mutant was impaired in its SG-inducing capability, indicating that the eIF4E–DDX3 interaction is critical for the SG-inducing ability of DDX3. Notably, because the eIF4E-binding-defective mutant DDX3^{L43A} is impaired in its ability to repress translation [12], these results provide a functional link between the translational inhibitory effect of DDX3 and its SG-inducing activity.

DDX3 enhances cell viability following stress

Several SG components, such as RSK2 (ribosomal S6 kinase 2), hnRNP (heterogeneous nuclear RNP) A1 and MLN51 (metastatic lymph node 51), participate in the stress response by increasing cell viability following stress [23–25]. To address the physiological role of DDX3 in stress response, DDX3

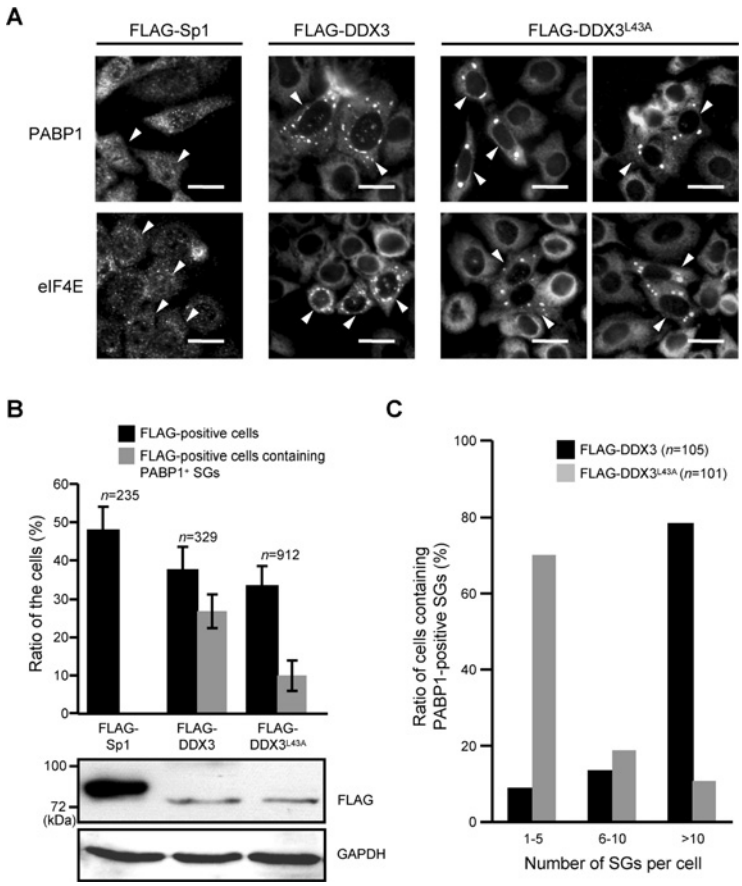

Figure 5 The eIF4E–DDX3 interaction is required for the SG-inducing ability of DDX3

(**A**) FLAG-tagged Sp1, DDX3 or DDX3^{L43A} was transiently expressed in HeLa cells. After 44 h, cells were fixed and immunostained for PABP1 or eIF4E. Counterstaining with anti-FLAG antibody is shown in Supplementary Figure S8 at http://www.BiochemJ.org/bj/441/bj4410119add.htm. The transfected cells (FLAG-positive) are marked by arrowheads. Scale bars, 20 μm. (**B**) Three independent immunofluorescence analyses showing the percentage of transfected cells (FLAG-positive) and the ratio of the transfected cells harbouring PABP1-positive SGs are quantified. Immunoblotting of the cell lysate was performed using antibodies against the indicated proteins. (*n*, the number of cells used for quantification). GAPDH, glyceraldehyde-3-phosphate dehydrogenase. Molecular masses are indicated in kDa. (**C**) The number of PABP1-positive SGs per cell was counted in the indicated plasmid-transfected cells harbouring SGs (*n*, the number of FLAG-positive cells harbouring SGs used for quantification).

knockdown cells were stressed with 1 M sorbitol for 1 h, and cell viability after stress release was evaluated. As shown in Figure 6(A), after transfection for 72 h, down-regulation of DDX3 had no obvious effect on cell viability before the induction of stress. However, DDX3-silenced cells lost viability significantly after osmotic stress release, indicating that DDX3 down-regulation reduces cell viability after osmotic stress. To validate that this poor recovery was due to the lack of DDX3, we complemented DDX3-silenced cells with a shRNA-insensitive DDX3 mutant. As shown in Figure 6(A), supplementation with shRNA-resistant FLAG–DDX3 could partially enhance the cell viability after osmotic stress in a dose-dependent manner. Similarly, DDX3 silencing produced a dose-dependent decrease in cell survival following oxidative stress induced by the treatment of 1 mM arsenite for 1 h (from 71 % to 43 %, Figure 6B). Notably, DDX3 overexpression alone could rescue cell viability after stress (see Supplementary Figure S9 at http://www.BiochemJ.org/bj/441/bj4410119add.htm). These results clearly indicate that DDX3 plays a role in the stress response by favouring cell recovery following stress, a feature in good agreement with its SG-inducing capability in stress response.

Because the eIF4E-binding defective mutant DDX3^{L43A} fails to induce SG assembly, we next investigate whether this eIF4E-binding ability and SG-inducing capability of DDX3 is relevant to its role in cell viability after stress. HeLa cells expressing ectopic wild-type DDX3 or eIF4E-binding-defective mutant DDX3^{L43A} were treated with arsenite and accessed for cell viability as described above. As shown in Figure 6(C), compared with wild-type DDX3, overexpression of DDX3^{L43A} mutant failed to rescue cell survival following oxidative stress as cell viability decreased from 88 % (wild-type DDX3) to 53 % (DDX3^{L43A}). This is a clear indication that the SG-inducing capability and the eIF4E-binding ability of DDX3 plays a pivotal role in cell viability under stress.

A recent study showed that SGs provide a protective role during stress by preventing apoptosis through sequestering apoptosis-promoting factors in SGs [2]. To clarify the underlying mechanism by which DDX3 aids cell survival, the effect of DDX3 on stress-induced apoptosis was examined. DDX3-knockdown cells were treated with arsenite, left to recover as described in the aforementioned viability assays and subsequently accessed for apoptosis by annexin V staining or detection of PARP proteolysis. It was shown that the DDX3 down-regulation-induced decline in cell viability after stress is, at least in part, due to an increase in apoptosis, as demonstrated by the increased levels of annexin V staining (Figure 6D) and PARP proteolysis (see Supplementary Figure S10 at

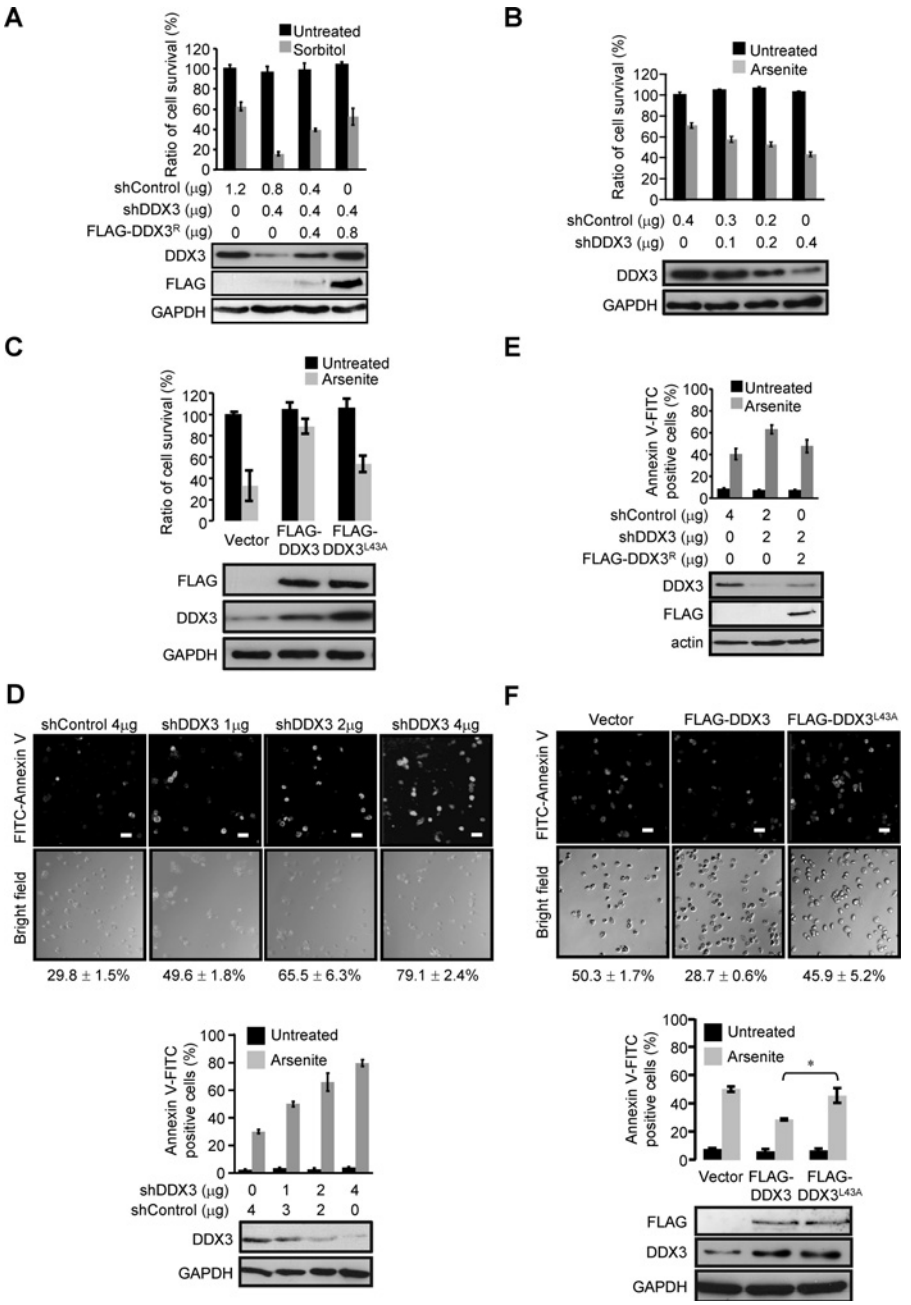

Figure 6 DDX3 increases cell survival following stresses

(**A**) DDX3 aids cell survival after osmotic stress. HeLa cells grown in the 12-well culture plate were transfected with the indicated plasmids. After 48 h, cells were treated with 1 M sorbitol for 1 h and left to recover for 24 h. Cell viability was then assessed by MTT assays. The relative cell survival of the control plasmid-transfected cells without stress stimulation is designated as 100%. Immunoblotting of the cell lysate was performed using specific antibodies as indicated. (**B**) Silencing DDX3 reduces cell viability following oxidative stress. HeLa cells grown in the 24-well culture plate were transfected with various amounts of DDX3-silencing plasmid as indicated. At 48 h post-transfection, cells were treated with 1 mM arsenite for 1 h. After recovery, cell viability was assessed and analysed as described above. Immunoblotting of the cell lysate showing the expression level of DDX3 is shown at the bottom. (**C**) The eIF4E-binding defective DDX3 mutant fails to restore cellular viability following oxidative stress. HeLa cells were transfected with the indicated plasmids. Cell viability after arsenite treatment was assessed as described above. Western blot analysis of the transfected cell lysates for the indicted proteins is shown at the bottom. (**D**) Silencing DDX3 enhances arsenite-induced apoptosis. HeLa cells were transfected with various amounts of DDX3-silencing plasmid as indicated. At 48 h post-transfection, cells were treated with 1 mM arsenite for 1 h. After recovery for 24 h, percentage of apoptotic cells was determined by annexin V staining. Results are means $\pm$ S.D. of three independent determinations. Representative immunohistochemistry from annexin V/FITC staining and brightfield is shown on the left. Western blot analysis of the transfected cell lysates for the expression of DDX3 is shown at the bottom. Scale bars, 40 μm. (**E**) Quantification of arsenite-induced apoptotic cells in HeLa cultures transfected with control vector, DDX3-silencing plasmid or together with shRNA-resistant FLAG–DDX3 as indicated. Apoptotic cells were induced and analysed as described in (**D**). (**F**) The wild-type DDX3, but not DDX3^{L43A} mutant, could suppress arsenite-induced apoptosis. HeLa cells were transfected with parental vector or expression constructs encoding various FLAG–DDX3 constructs as indicated, then treated with arsenite and analysed as described in (**D**). *$P < 0.05$. GAPDH, glyceraldehyde-3-phosphate dehydrogenase.

http://www.BiochemJ.org/bj/441/bj4410119add.htm). In addition, restoring with shRNA-insensitive FLAG–DDX3 could partially reduce the enhanced ratio of apoptotic cells in DDX3-knockdown cultures (Figure 6E). This DDX3-induced apoptotic resistance after stress is in good agreement with the SG-inducing ability of DDX3. Furthermore, the failure of the DDX3^{L43A} mutant to rescue cell viability after stress results from an inability to exert its apoptosis resistant effect, as shown by the increased levels of annexin V staining (Figure 6F, 46 % compared with 29 %) and PARP proteolysis (see Supplementary Figure S11 at http://www.BiochemJ.org/bj/441/bj4410119add.htm) in DDX3^{L43A}-expressing cells after arsenite treatment. These results support further the notion that DDX3 suppresses stress-induced apoptosis through inducing SG assembly. Taken together, these findings show that DDX3 plays a broad role in the stress response through involvement in SG assembly and cell recovery. As the eIF4E–DDX3 interaction is shown to be required for DDX3-mediated translational suppression, SG assembly and cell recovery under adverse conditions, the present study provides a novel mechanistic insight into the integral roles of DDX3 and eIF4E in co-ordinating translational regulation with stress response.

DISCUSSION

In the present study, we described co-ordinative roles for RNA helicase DDX3 and its interactions with eIF4E/PABP1 in SG assembly and stress response. A wide variety of stress stimuli direct DDX3 together with eIF4E and PABP1 into cytoplasmic SGs (Figure 1), revealing a general role of DDX3 in SG physiology. Consistent with this notion, DDX3 actively participates in SG formation as down-regulation of DDX3 impaired stress-induced SG formation, whereas the supplementation of shRNA-resistant FLAG–DDX3 could restore this defect (Figure 2). Also noted, DDX3 overexpression induced SG formation in a concentration-dependent manner (see Supplementary Figure S5) as reported for other SG-nucleating components. Therefore DDX3 should be added to a growing list of SG core constitutes. Currently, five RNA helicases, DDX1, DDX3, DDX6 (rck/p54), RHAU and eIF4A, have been shown to localize in SGs [2]. To our knowledge, DDX3 is perhaps the first RNA helicase reported to function as an SG-nucleating factor and an integral component for stress response.

The precise mechanism by which DDX3 induces SG formation remains to be defined. Considering the interactions of DDX3 with PABP1 (Figure 1A) and with other SG components [such as eIF4E, eIF4A and TDRD3 (Tudor domain-containing 3)] [12,13,17], it is possible that DDX3 may serve as a scaffold and form multimeric complex in SGs. Among these interacting factors, DDX3 is the first one reported to harbour SG-inducing ability. These results indentify DDX3 as a good candidate to mediate other factors into SGs. Although the SG-inducing ability of DDX3 is independent of its ATPase and helicase activities (Figure 3), whether these enzymatic activities are necessary for other functions of DDX3 in SGs remains to be determined. Most remarkably, we demonstrated that the interaction between eIF4E and DDX3 is a prerequisite for the assembly of DDX3-induced SGs, as the absence of the eIF4E-binding motif within DDX3 or a point mutation within this eIF4E-binding consensus sequence led to a defect in the SG formation process (Figures 4 and 5). Previously, we showed that DDX3 utilizes this eIF4E-binding domain to trap eIF4E in a translationally inactive complex and represses cap-dependent translation [12]. Therefore the SG induction could be one of the consequences of the inhibitory effect of DDX3 overexpression on translation. In addition, because the eIF4E-binding-defective mutant DDX3^{L43A} is impaired in its ability to repress translation [12], the requirement of eIF4E–DDX3 interaction for SG-inducing ability of DDX3 provides a functional link between the translational-inhibitory effect of DDX3 and its SG-inducing activity. Given that depletion of eIF4E or preventing its interaction with eIF4G could lead to SG formation [26], an excess of DDX3 could sequester eIF4E, leading to the accumulation of abortive translation pre-initiation complex, and thereby facilitates SG assembly in a similar manner to other SG-promoting translational regulators, such as FMRP (fragile X mental retardation protein), CPEB1 (cytoplasmic polyadenylation element-binding protein 1), Smaug and Pumilio 2 [1].

The present study demonstrated the direct interaction between DDX3 and PABP1 (Figure 1A). This DDX3–PABP1 interaction may provide new insight into the mRNP structure within SGs. Several observations argue that not all mRNPs within SGs form the classical 48S complex containing the closed loop structure of mRNA linked by eIF4E, eIF4G and PABP1 [2]. Our previous study demonstrated that DDX3 could efficiently compete with eIF4G for eIF4E binding [12]. Considering the direct interactions of DDX3 with eIF4E and PABP1, one possible scenario is that DDX3, eIF4E and PABP1 may form an alternative molecular bridge between both ends of the mRNA to maintain RNA stability in DDX3-facilitated SGs. In contrast with SGs, PBs exist constitutively for mRNA degradation. Our results demonstrate that, under oxidative or osmotic stress, DDX3 does not migrate into PBs (Figure 1E). Thus DDX3 could be considered as a specific marker of SGs. In addition, the shuttle of mRNAs between SGs and PBs implies transitions between different mRNP states [2,27]. This process may be facilitated by RNA helicases. Therefore the presence of DDX3 in the juxtaposition of SGs and PBs (Figure 1E) suggests a possible role for DDX3 in the mRNP remodelling at the interface between these two structures.

A previous study reported that knockdown of DDX3 did not impair arsenite-induced SG assembly [13]. Another screening work using RNAi (RNA interference) technology identified 101 human genes required for arsenite-induced SG assembly, except for DDX3 [28]. DDX3 was not identified in these studies, probably due to failure to completely deplete the endogenous DDX3 and residual SGs occasionally seen in some cells (Figure 2). Interestingly, DDX3 knockdown also results in the nuclear accumulation of PABP1, whereas supplementation with shRNA-insensitive FLAG–DDX3 recovered the translocation of PABP1 into SGs (Figure 2B). PABP1 has also been shown to relocate into the nucleus during rotavirus and herpesvirus infection [29,30]. In addition, as viral protein translation is absolutely dependent on the functional host protein synthesis machinery, the fundamental role of SGs in the stress response suggests that these complexes may provide another arm of the innate immunity by affecting the metabolism of viral mRNAs and restricting viral infections [31]. Accordingly, it seems that rotavirus changes the intracellular localization of SG components such as PABP1 and prevents SG assembly to allow the translation of its mRNAs [29]. A number of human viral pathogens were found to repress or induce SG formation depending on their particular replication requirements [1]. Considering that DDX3 is reported to be required for virus replication [7,32], the interplay between virus and DDX3-mediated SG assembly would be an interesting issue to address.

In the present study, we also showed that cells lacking DDX3, consequently impaired in SG formation, fail to recover properly from stress and undergo apoptosis (Figure 6). DDX3 has been identified as a constitute of an anti-apoptotic protein complex at death receptors [33]. In the present paper, we describe a novel role for DDX3 in ensuring cell viability during the response to stress. Furthermore, this protective effect relies, at least partially, on the

interaction between DDX3 and eIF4E (Figure 6), illustrating coordinative roles and action mechanisms for DDX3 in translation control, SG assembly and cell survival upon environmental insults. In conclusion, the present study characterizes the RNA helicase DDX3 as a critical component of SGs and provides a molecular framework for envisaging the functional roles of DDX3, eIF4E and PABP1 in SGs formation and stress response.

AUTHOR CONTRIBUTION

Jing-Wen Shih was primarily responsible for experimental design, data acquisition, data analysis and the preparation of the paper. Wei-Ting Wang generated EGFP–DDX3 variant constructs and participated in the initial characterization of DDX3 in SGs upon heat shock with Chu-Yun Kuo and Tsung-Yuan Tsai. Tsung-Yuan Tsai prepared samples for the MS analysis and provided technical assistance. Hao-Kang Li designed and cloned the shRNA-resistant construct. Yan-Hwa Wu Lee supervised the project, obtained grant support and edited the paper before submission.

ACKNOWLEDGEMENTS

We thank Dr Yeou-Guang Tsay for assistance with MS analysis and the National RNAi Core Facility (Taiwan) for the shRNA vector.

FUNDING

This work was supported by the National Science Council [grant numbers NSC-97-2320-B-010-014-MY3, NSC-98-2320-B-010-007-MY3, NSC-97-2320-B-009-003-MY3 and NSC-98-2320-B-009-003-MY3 (to Y.-H.W.L.)], the National Health Research Institute [grant numbers NHRI-EX98-9501BI and NHRI-EX99-9501BI (to Y.-H.W.L.)] and the Ministry of Education of the Republic of China 'Aim for the Top University Plan' [grant number 99A-C-P501 (to Y.-H.W.L.)].

REFERENCES

1 Anderson, P. and Kedersha, N. (2008) Stress granules: the Tao of RNA triage. Trends Biochem. Sci. **33**, 141–150
2 Buchan, J. R. and Parker, R. (2009) Eukaryotic stress granules: the ins and outs of translation. Mol. Cell **36**, 932–941
3 Anderson, P. and Kedersha, N. (2009) Stress granules. Curr. Biol. **19**, R397–R398
4 Kedersha, N., Stoecklin, G., Ayodele, M., Yacono, P., Lykke-Andersen, J., Fritzler, M. J., Scheuner, D., Kaufman, R. J., Golan, D. E. and Anderson, P. (2005) Stress granules and processing bodies are dynamically linked sites of mRNP remodeling. J. Cell Biol. **169**, 871–884
5 Rocak, S. and Linder, P. (2004) DEAD-box proteins: the driving forces behind RNA metabolism. Nat. Rev. Mol. Cell Biol. **5**, 232–241
6 Cordin, O., Banroques, J., Tanner, N. K. and Linder, P. (2006) The DEAD-box protein family of RNA helicases. Gene **367**, 17–37
7 Yedavalli, V. S., Neuveut, C., Chi, Y. H., Kleiman, L. and Jeang, K. T. (2004) Requirement of DDX3 DEAD box RNA helicase for HIV-1 Rev-RRE export function. Cell **119**, 381–392
8 You, L. R., Chen, C. M., Yeh, T. S., Tsai, T. Y., Mai, R. T., Lin, C. H. and Wu Lee, Y. H. (1999) Hepatitis C virus core protein interacts with cellular putative RNA helicase. J. Virol. **73**, 2841–2853
9 Kanai, Y., Dohmae, N. and Hirokawa, N. (2004) Kinesin transports RNA: isolation and characterization of an RNA-transporting granule. Neuron **43**, 513–525
10 Zhou, Z., Licklider, L. J., Gygi, S. P. and Reed, R. (2002) Comprehensive proteomic analysis of the human spliceosome. Nature **419**, 182–185
11 Chao, C. H., Chen, C. M., Cheng, P. L., Shih, J. W., Tsou, A. P. and Wu Lee, Y. H. (2006) DDX3, a DEAD box RNA helicase with tumor growth-suppressive property and transcriptional regulation activity of the *p21*$^{waf1/cip1}$ promoter, is a candidate tumor suppressor. Cancer Res. **66**, 6579–6588
12 Shih, J. W., Tsai, T. Y., Chao, C. H. and Wu Lee, Y. H. (2008) Candidate tumor suppressor DDX3 RNA helicase specifically represses cap-dependent translation by acting as an eIF4E inhibitory protein. Oncogene **27**, 700–714
13 Lai, M. C., Lee, Y. H. and Tarn, W. Y. (2008) The DEAD-box RNA helicase DDX3 associates with export messenger ribonucleoproteins as well as tip-associated protein and participates in translational control. Mol. Biol. Cell **19**, 3847–3858
14 Lai, M. C., Chang, W. C., Shieh, S. Y. and Tarn, W. Y. (2010) DDX3 regulates cell growth through translational control of cyclin E1. Mol. Cell. Biol. **30**, 5444–5453
15 Lee, C. S., Dias, A. P., Jedrychowski, M., Patel, A. H., Hsu, J. L. and Reed, R. (2008) Human DDX3 functions in translation and interacts with the translation initiation factor eIF3. Nucleic Acids Res. **36**, 4708–4718
16 Tarn, W. Y. and Chang, T. H. (2009) The current understanding of Ded1p/DDX3 homologs from yeast to human. RNA Biol. **6**, 17–20
17 Goulet, I., Boisvenue, S., Mokas, S., Mazroui, R. and Cote, J. (2008) TDRD3, a novel Tudor domain-containing protein, localizes to cytoplasmic stress granules. Hum. Mol. Genet. **17**, 3055–3074
18 Kedersha, N. and Anderson, P. (2007) Mammalian stress granules and processing bodies. Methods Enzymol. **431**, 61–81
19 Chang, P. C., Chi, C. W., Chau, G. Y., Li, F. Y., Tsai, Y. H., Wu, J. C. and Wu Lee, Y. H. (2006) DDX3, a DEAD box RNA helicase, is deregulated in hepatitis virus-associated hepatocellular carcinoma and is involved in cell growth control. Oncogene **25**, 1991–2003
20 Tsai, N. P., Ho, P. C. and Wei, L. N. (2008) Regulation of stress granule dynamics by Grb7 and FAK signalling pathway. EMBO J. **27**, 715–726
21 Beckham, C., Hilliker, A., Cziko, A. M., Noueiry, A., Ramaswami, M. and Parker, R. (2008) The DEAD-box RNA helicase Ded1p affects and accumulates in *Saccharomyces cerevisiae* P-bodies. Mol. Biol. Cell **19**, 984–993
22 Tanner, N. K. and Linder, P. (2001) DExD/H box RNA helicases: from generic motors to specific dissociation functions. Mol. Cell **8**, 251–262
23 Baguet, A., Degot, S., Cougot, N., Bertrand, E., Chenard, M. P., Wendling, C., Kessler, P., Le Hir, H., Rio, M. C. and Tomasetto, C. (2007) The exon-junction-complex-component metastatic lymph node 51 functions in stress-granule assembly. J. Cell Sci. **120**, 2774–2784
24 Eisinger-Mathason, T. S., Andrade, J., Groehler, A. L., Clark, D. E., Muratore-Schroeder, T. L., Pasic, L., Smith, J. A., Shabanowitz, J., Hunt, D. F., Macara, I. G. and Lannigan, D. A. (2008) Codependent functions of RSK2 and the apoptosis-promoting factor TIA-1 in stress granule assembly and cell survival. Mol. Cell **31**, 722–736
25 Guil, S., Long, J. C. and Caceres, J. F. (2006) hnRNP A1 relocalization to the stress granules reflects a role in the stress response. Mol. Cell. Biol. **26**, 5744–5758
26 Mokas, S., Mills, J. R., Garreau, C., Fournier, M. J., Robert, F., Arya, P., Kaufman, R. J., Pelletier, J. and Mazroui, R. (2009) Uncoupling stress granule assembly and translation initiation inhibition. Mol. Biol. Cell **20**, 2673–2683
27 Anderson, P. and Kedersha, N. (2009) RNA granules: post-transcriptional and epigenetic modulators of gene expression. Nat. Rev. Mol. Cell Biol. **10**, 430–436
28 Ohn, T., Kedersha, N., Hickman, T., Tisdale, S. and Anderson, P. (2008) A functional RNAi screen links O-GlcNAc modification of ribosomal proteins to stress granule and processing body assembly. Nat. Cell Biol. **10**, 1224–1231
29 Montero, H., Rojas, M., Arias, C. F. and Lopez, S. (2008) Rotavirus infection induces the phosphorylation of eIF2α but prevents the formation of stress granules. J. Virol. **82**, 1496–1504
30 Salaun, C., MacDonald, A. I., Larralde, O., Howard, L., Lochtie, K., Burgess, H. M., Brook, M., Malik, P., Gray, N. K. and Graham, S. V. (2010) Poly(A)-binding protein 1 partially relocalizes to the nucleus during herpes simplex virus type 1 infection in an ICP27-independent manner and does not inhibit virus replication. J. Virol. **84**, 8539–8548
31 Schutz, S. and Sarnow, P. (2007) How viruses avoid stress. Cell Host Microbe **2**, 284–285
32 Ariumi, Y., Kuroki, M., Abe, K., Dansako, H., Ikeda, M., Wakita, T. and Kato, N. (2007) DDX3 DEAD-box RNA helicase is required for hepatitis C virus RNA replication. J. Virol. **81**, 13922–13926
33 Sun, M., Song, L., Li, Y., Zhou, T. and Jope, R. S. (2008) Identification of an antiapoptotic protein complex at death receptors. Cell Death Differ. **15**, 1887–1900

Received 26 April 2011/22 August 2011; accepted 1 September 2011
Published as BJ Immediate Publication 1 September 2011, doi:10.1042/BJ20110739

Biochem. J. (2012) **441**, 119–129 (Printed in Great Britain) doi:10.1042/BJ20110739

SUPPLEMENTARY ONLINE DATA

Critical roles of RNA helicase DDX3 and its interactions with eIF4E/PABP1 in stress granule assembly and stress response

Jing-Wen SHIH*, Wei-Ting WANG*, Tsung-Yuan TSAI*, Chu-Yun KUO*, Hao-Kang LI* and Yan-Hwa WU LEE*†

*Institute of Biochemistry and Molecular Biology, National Yang Ming University, Taipei 112, Taiwan, and †Department of Biological Science and Technology, National Chiao Tung University, Hsinchu 300, Taiwan

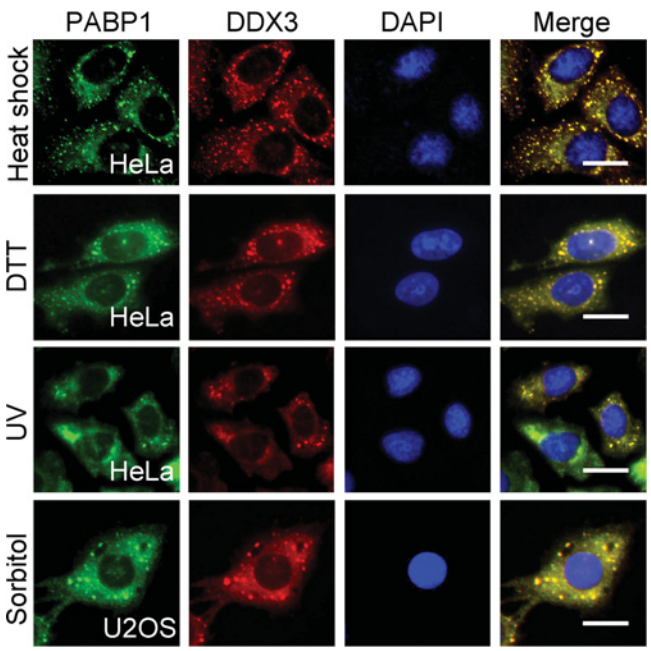

Figure S1 DDX3 migration into SGs is induced by various environmental stresses

HeLa or U2OS cells were exposed to heat shock, endoplasmic reticulum stress (1 mM DTT), UV irradiation or high-osmolarity medium (1 M sorbitol for 30 min). The cells were fixed and immunostained for PABP1 and DDX3. Scale bars, 20 μm. DAPI, 4′,6-diamidino-2-phenylindole.

[1] To whom correspondence should be addressed (email yhwulee@nctu.edu.tw).

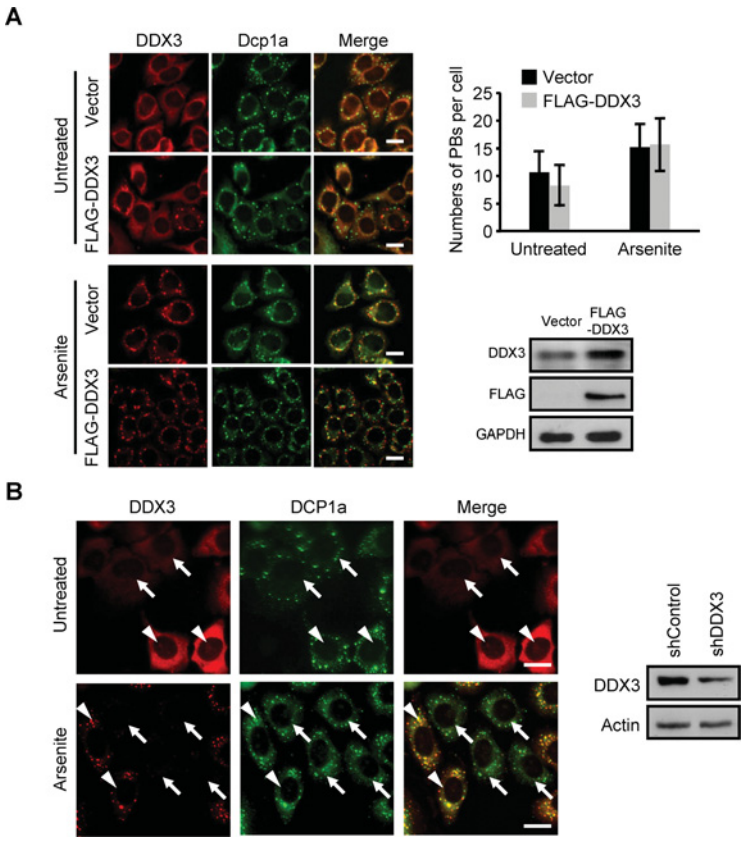

Figure S2 DDX3 has little effect on PB formation

(**A**) Effect of DDX3 overexpression on the integrity of PB assembly. HeLa cells were transiently transfected with vector or FLAG–DDX3 expression plasmid, then cultured in the absence or presence of 0.5 mM sodium arsenite for 30 min. After fixation, endogenous DDX3 and Dcp1 (a marker of PBs) were detected by immunofluorescence microscopy. PBs were quantified by counting at least 100 cells from two independent experiments for each condition. Results are means $\pm$ S.D. Western blot analysis of the transfected cell lysates (50 μg) for the expression of exogenous DDX3 is shown in the bottom right. Scale bars, 20 μm. GAPDH, glyceraldehyde-3-phosphate dehydrogenase. (**B**) Effect of DDX knockdown on PB integrity. HeLa cells were transiently transfected with control vector (shControl) or DDX3-silencing plasmid (shDDX3), then cultured in the absence or presence of 0.5 mM sodium arsenite for 30 min. Immunohistochemistry of DDX3 and Dcp1a in DDX3-silenced HeLa cells is shown as indicated. Efficiently and inefficiently silenced cells are marked by arrows and arrowheads respectively. Western blot analysis of the transfected cell lysates (50 μg) for the expression of DDX3 is shown. Scale bars, 20 μm.

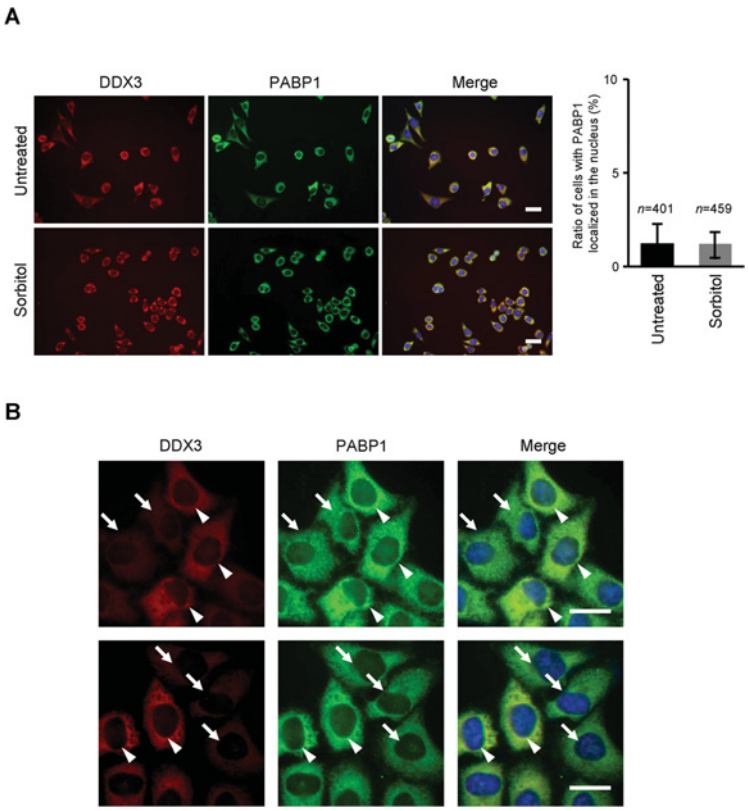

Figure S3 Neither sorbitol treatment nor DDX3 knockdown alone could induce nuclear accumulation of PABP1

(**A**) Effect of sorbitol treatment on the relocalization of PABP1 into the nucleus. Immunohistochemistry of PABP1 and DDX3 in HeLa cells before (untreated) or after (Sorbitol) sorbitol treatment are shown. The nucleus is shown in blue in the merged images by DAPI (4′,6-diamidino-2-phenylindole) staining. Quantification of cells with PABP1 localized in the nucleus is shown on the right. Scale bars, 40 μm. (*n*, the number of cells used for quantification). (**B**) Effect of DDX knockdown on the distribution of PABP1. Immunohistochemistry of DDX3 and PABP1 in DDX3-silenced HeLa cells is shown. Efficiently and inefficiently silenced cells are marked by arrows and arrowheads respectively. The nucleus is shown in blue in the merged images by DAPI staining. Scale bars, 20 μm.

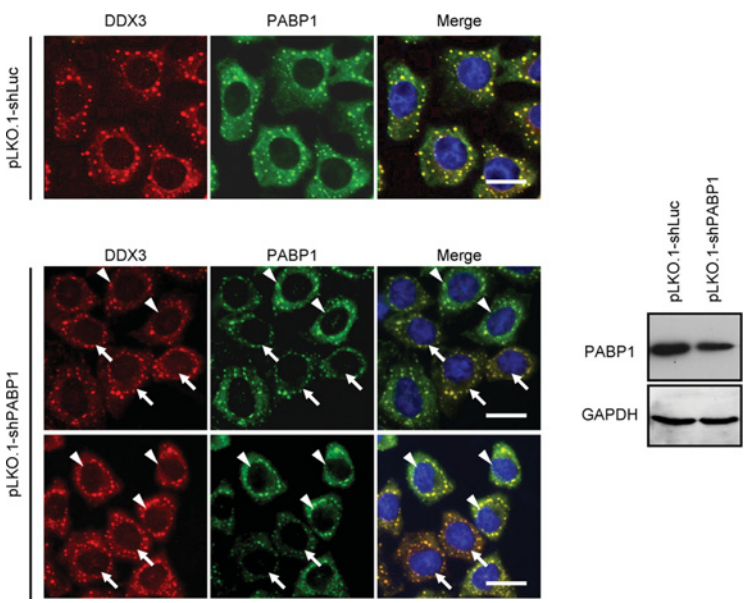

Figure S4 PABP1 knockdown has little effect on SG formation

Effect of PABP1 knockdown on SG integrity. HeLa cells were transiently transfected with control vector (pLKO.1-shLuc) or PABP1-silencing plasmid (pLKO.1-shPABP1), then cultured in the presence of 0.5 mM sodium arsenite for 30 min. Immunohistochemistry of DDX3 and PABP1 in transfected HeLa cells is shown. The nucleus is shown in blue in the merged images by DAPI (4′,6-diamidino-2-phenylindole) staining. Efficiently and inefficiently silenced cells are marked by arrows and arrowheads respectively. Western blot analysis of the transfected cell lysates (50 μg) for the expression of PABP1 is shown on the right. Scale bars, 20 μm. GAPDH, glyceraldehyde-3-phosphate dehydrogenase.

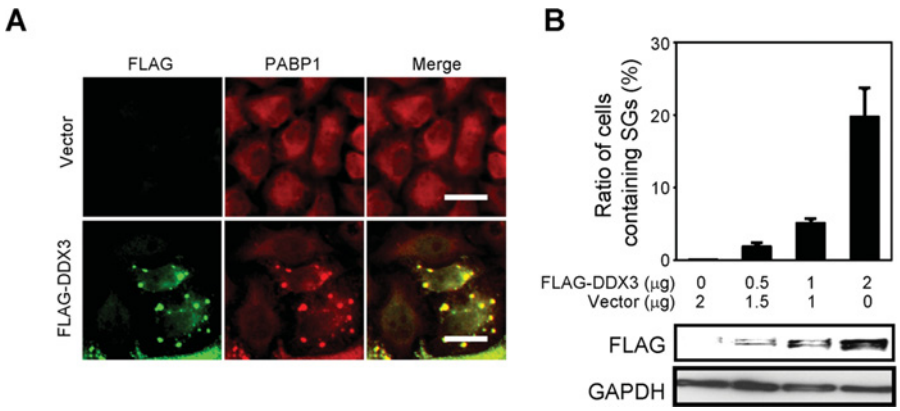

Figure S5 DDX3 is a SG nucleator

(**A**) Overexpression of DDX3 is sufficient for SG induction. HeLa cells were transiently transfected with vector or expression plasmids encoding FLAG–DDX3. After 24 h, immunostaining was carried out using anti-FLAG and anti-PABP1 antibodies. Scale bar, 20 μm. (**B**) Overexpression of DDX3 induces SG assembly in a dose-dependent manner. HeLa cells grown on cover slips in the six-well culture plate were transfected with vector and/or FLAG–DDX3 expression plasmid as indicated. At 24 h post-transfection, immunostaining was performed using anti-DDX3 antibody to visualize SGs. At least 200 cells were counted for each condition. The percentage of transfected cells harbouring SGs was quantified. Each experiment was performed in triplicate. GAPDH, glyceraldehyde-3-phosphate dehydrogenase.

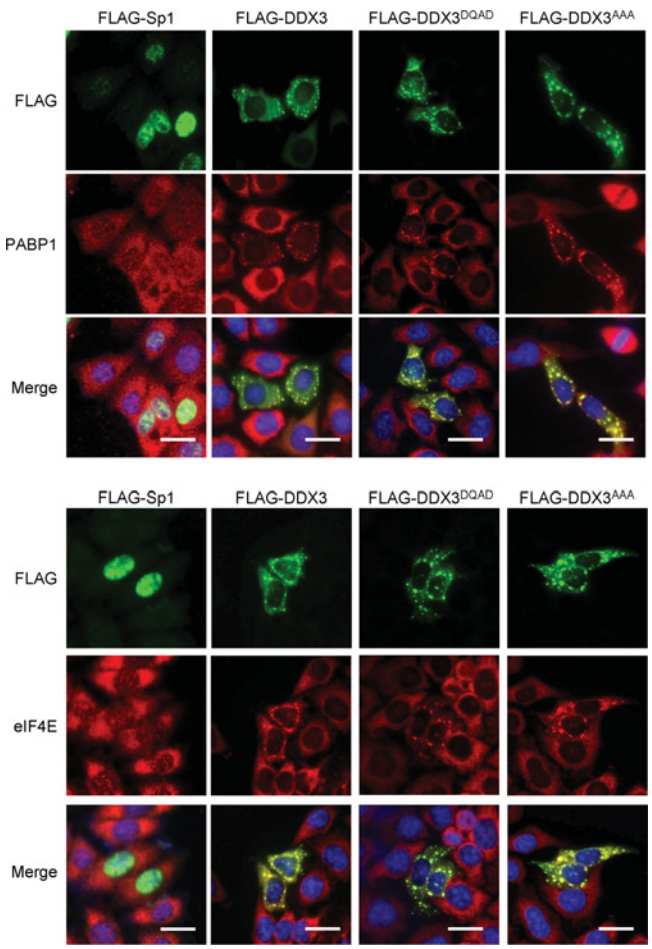

Figure S6 Overexpression of DDX3, DDX3^{DQAD} or DDX3^{AAA} mutants induced PABP1- and eIF4E-containing SG assembly without stress treatment

FLAG-tagged Sp1, DDX3, DDX3^{DQAD} or DDX3^{AAA} was transiently expressed in HeLa cells. Immunostaining was performed using antibodies against FLAG with PABP1 or eIF4E. The nucleus is shown in blue in the merged images by DAPI (4′,6-diamidino-2-phenylindole) staining. Scale bars, 20 μm.

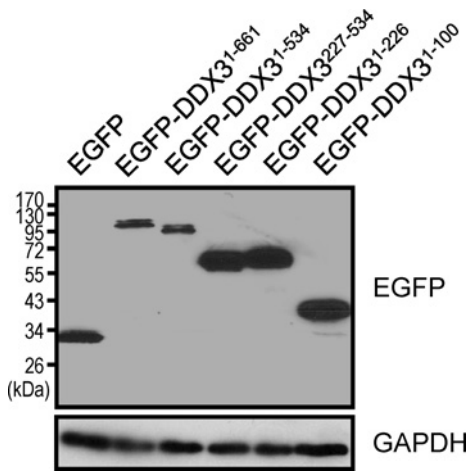

Figure S7 Western blot analysis of exogenous DDX3 fragments expression in HeLa cells

HeLa cells were transfected with the expression constructs as indicated. The expression of exogenous EGFP–DDX3 fragments were detected with an anti-EGFP antibody. GAPDH, glyceraldehyde-3-phosphate dehydrogenase. Molecular masses are indicated in kDa.

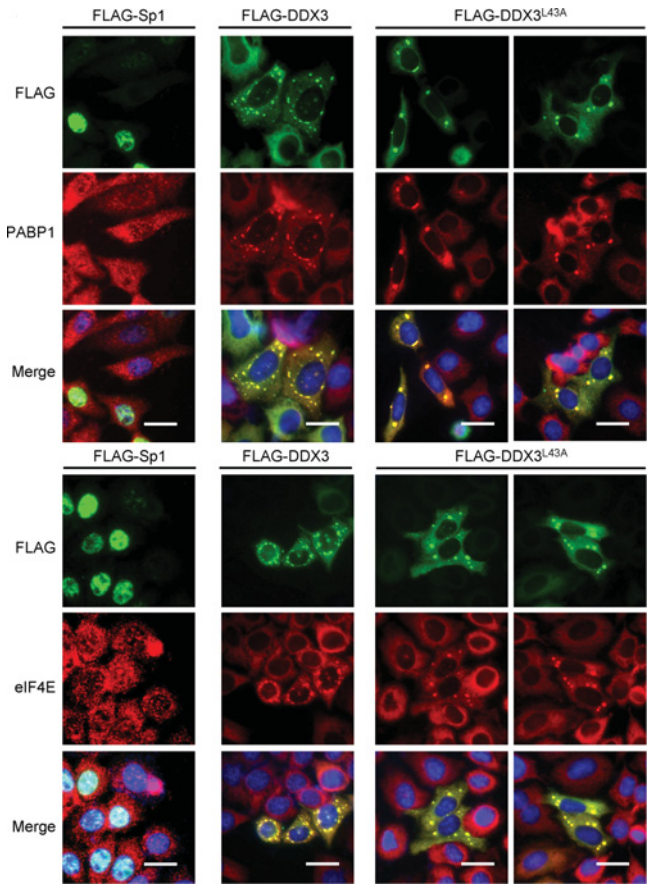

Figure S8 Overexpression of DDX3^{L43A} mutant induced less PABP1- and eIF4E-containing SGs than wild-type DDX3

FLAG-tagged Sp1, DDX3 or DDX3^{L43A} was transiently expressed in HeLa cells. Immunostaining was performed using antibodies against FLAG with PABP1 or eIF4E. The nucleus is shown in blue in the merged images by DAPI (4′,6-diamidino-2-phenylindole) staining. Scale bars, 20 μm.

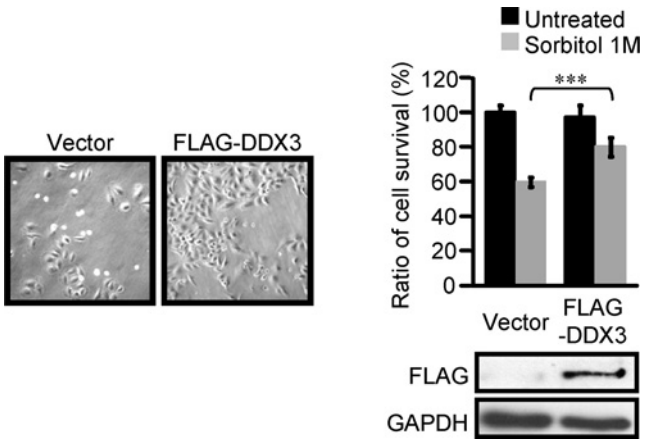

Figure S9 Overexpression of DDX3 increases cell viability following osmotic stress

HeLa cells were transfected with control plasmid or FLAG–DDX3 expression construct. At 48 h post-transfection, cells were left untreated or stressed with 1 M sorbitol for 1 h. After recovery in normal medium for 24 h, cell viability was assessed by cell counting and normalized to that of the untreated control plasmid transfectants. $^{***}P < 0.001$. GAPDH, glyceraldehyde-3-phosphate dehydrogenase. Left-hand panels show the morphology of the transfected cells as indicated after osmotic stress.

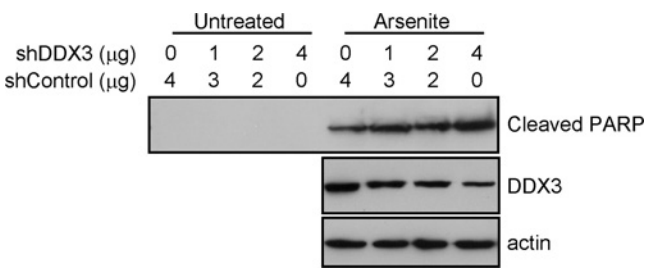

Figure S10 DDX3 silencing enhances arsenite-induced apoptosis

HeLa cells were transfected with various amounts of DDX3-silencing plasmid as indicated. At 48 h post-transfection, cells were treated with 1 mM sodium arsenite for 1 h. After recovery for 24 h, PARP proteolysis was measured by immunoblot analysis with an antibody against cleaved PARP.

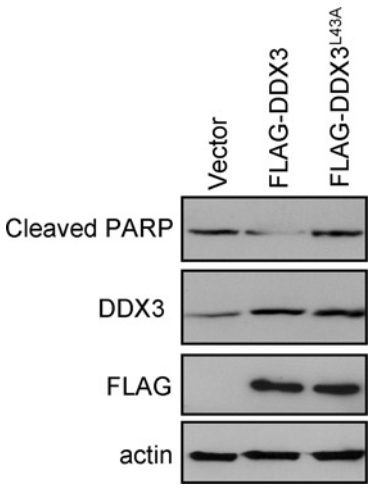

Figure S11 Wild-type DDX3, but the not DDX3^{L43A} mutant, could suppress arsenite-induced apoptosis

HeLa cells were transfected with parental vector or expression constructs encoding various FLAG–DDX3 as indicated. At 48 h post-transfection, cells were treated with 1 mM sodium arsenite for 1 h. After recovery for 24 h, PARP proteolysis was measured by immunoblot analysis with an antibody against cleaved PARP.

Received 26 April 2011/22 August 2011; accepted 1 September 2011
Published as BJ Immediate Publication 1 September 2011, doi:10.1042/BJ20110739